Phosphorylation of the cAMP Response Element Binding Protein CREB by cAMP-Dependent Protein Kinase A and Glycogen Synthase Kinase-3 Alters DNA-Binding Affinity, Conformation, and Increases Net Charge

Bryant P. Bullock and Joel F. Habener*

Laboratory of Molecular Endocrinology, Massachusetts General Hospital and Howard Hughes Medical Institute, Harvard Medical School, Boston, Massachusetts 02114

Received April 25, 1997; Revised Manuscript Received January 6, 1998

ABSTRACT: The cAMP response element binding protein CREB activates the transcription of genes in response to phosphorylation by cAMP-dependent protein kinase A (PKA) and other protein kinases. Phosphorylated CREB activates transcription by recruiting transcriptional co-activators such as the CREB binding protein. Here, we describe experiments that analyze the effects of phosphorylation on the DNA binding affinity of CREB and the structural characteristics of the CREB/DNA complex in solution. Analysis of deletion mutants of CREB indicate that amino acid sequences within the transactivation domain promote high-affinity binding of CREB to fluorescently labeled oligonucleotides containing cAMP response elements. In vitro experiments indicate that phosphorylation is processive between PKA as the initial kinase and glycogen synthase kinase-3 (GSK-3) but not casein kinase II as the secondary kinase. Fluorescent electrophoretic mobility shift assays show that phosphorylation by PKA results in a 3−5-fold increase in the binding affinity of CREB to both the symmetrical somatostatin CRE (SMS-CRE) and the asymmetric somatostatin upstream element (SMS-UE). Processive phosphorylation of CREB by GSK-3 attenuates the enhanced DNA binding in response to PKA thus acts as an inhibitor of PKA-induced binding. Ferguson plot analyses demonstrate that phosphorylation of CREB by PKA and GSK-3 result in an increase in the spherical size and the net positive surface charge of the CREB/DNA complex. Moreover, these analyses uncovered the unexpected finding that CREB associates as a tetramer both in the presence and absence of DNA. These findings suggest a model by which phosphorylation of CREB alters the secondary structure and charge characteristics of the CREB/DNA complex resulting in an alteration in binding affinity.

In response to environmental signals such as hormones, the cellular second messenger cyclic-AMP (cAMP) regulates a wide variety of metabolic processes, including gene transcription (Habener 1990; Lee & Masson 1993). Located within the promoters of cAMP responsive genes are specific DNA sequences, cyclic-AMP response elements (CREs), that bind specific proteins, including the CREB/ATF family of transcription factors, resulting in cAMP-activated transcription. The cAMP response element binding proteins CREB 327 and its isoform, CREB 341, are members of the bZIP family of transcriptional factors, characterized as bipartite proteins containing a carboxyl-terminal basic region-leucine zipper required for dimerization and DNA binding along with an amino-terminal transactivation domain (Hoeffler et al., 1988; Gonzalez et al., 1989).[1] Within the transactivation domain of CREB 327 is a region of approximately 45 amino acids (residues 92−137), the phosphorylation box (P-box) or kinase inducible domain (KID), which contains consensus phosphorylation motifs for several recognized protein kinases. The best characterized sequence is ^{116}RRPSY^{120} that is phosphorylated on serine 119 by several protein kinases including the cAMP-dependent protein kinase A (PKA), protein kinase C, calcium-calmodulin dependent kinase IV, the CREB kinase RSK-2, and the stress-activated kinase P38 (Yamamoto et al., 1988; Sheng et al., 1991; Ginty et al., 1994; Tan et al., 1996; Wilson et al., 1996). Phosphorylation at this serine is a prerequisite for transcriptional activation by cAMP signaling (Gonzalez & Montminy 1989; Habener et al., 1995). Mutation of serine 119, or serine 133 in the CREB 341 isoform, results in a complete loss of transactivational activities and the mutated protein acts as a dominant negative regulator of phosphoCREB (Gonzalez & Montminy 1989; Habener et al., 1995). Phosphorylation of CREB at serine 119 activates transcription by recruiting and associating with the transcriptional co-activator, CREB binding protein (CBP), leading to an interaction with the TFII? component of the basal transcription machinery resulting in the activation of RNA polymerase II directed gene transcription (Chrivia et al., 1993; Kwok et al., 1994).

In addition to the site phosphorylated by PKA, the P-box contains consensus sites for other serine/threonine protein kinases, such as glycogen synthase kinase-3 (GSK-3), casein kinase I and II (CK I and II), and Ca^{2+}/calmodulin kinase

* To whom correspondence should be addressed: Laboratory of Molecular Endocrinology, Massachusetts General Hospital−WEL320, 50 Blossom Street, Boston, MA 02114. Tel: (617) 726-5190. Fax: (617) 726-6954. E-mail: habenerj@a1.mgh.harvard.edu.

[1] The protein numbering scheme refers to the CREB 327 isoform lacking the alternatively spliced exon D that encodes 14 amino acids which is present in the CREB 341 isoform. Thus, serine 119 and serine 133 are equivalent among the two isoforms [see Habener et al. (1995)].

S0006-2960(97)00982-3 CCC: $15.00
Published on Web 02/25/1998

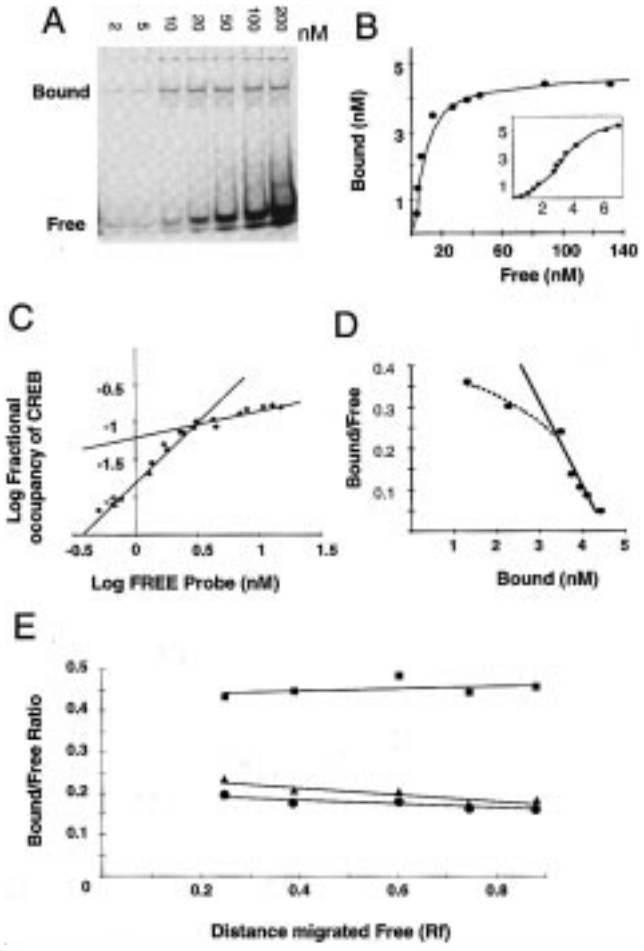

FIGURE 1: Fluorescent gel shift assay used to determine the binding affinity of CREB for the SMS-CRE. (A) A scan of a nondenaturing polyacrylamide gel on which 1 pmol of bacterial expressed CREB was titered with various amounts (2−200 nM) of a fluorescently tagged oligonucleotide containing the SMS-CRE. Following electrophoresis the gel was scanned with a single pass on a Molecular Dynamics 575 FluorImager using a PMT voltage of 700 and 100 micron resolution. The bound and free oligonucleotide probe is shown. (B) A saturation curve of the averages of eleven independent experiments of CREB binding to the SMS-CRE. Concentration of bound fluorescent oligonucleotide (nM) is plotted against the concentration of free oligonucleotide (nM). Inset shows the sigmoidal curve at low concentrations from a representative experiment. (C) Hill plot from the results of three independent experiments of 1 pmol of CREB binding to (20−0.5 nM) of F-SMS-CRE. Log of fractional occupancy of CREB is plotted against the log of Free probe. (D) Scatchard plot of the same results shown in Figure 1B. Bound vs free ratio is plotted against the concentration of bound fluorescent oligonucleotide (nM). The broken line represents the actual nonlinear curve while the solid line is the extrapolated curve used to calculate the binding constant. (E) A plot of the bound/free ratio of CREB (circles, squares) or PKA/GSK-3 phosphorylated CREB (triangles) binding to 250 nM (squares) or 100 nM (circles, triangles) of F-SMS-CRE versus the distance the free species migrated during a 90 min run on a nondenaturing electrophoresis gel (7%). The gel was scanned and the R_fs and relative quantities were calculated every 15 min.

(CamK) (Gonzalez et al., 1989; Habener et al., 1995). The P-box is divided into three separate domains (Figure 3A), PDE-1 (aa 92−108), PDE-2 (aa 121−131), and PDE-3 (aa 131−141), dependent on the consensus kinase motifs (Habener et al., 1995) of which one (PDE-1) is a focus in the studies described herein. Located adjacent to the PKA site at serine 115 is a consensus site for GSK-3 (^{115}SRRPS^{119}), a processive kinase site that requires an initial phosphorylation of serine 119 (Fiol et al., 1987, 1990; Roach 1991). Fiol and colleagues demonstrated that processive phosphorylation by PKA and GSK-3 occurred at these two serines within the CREB P-box resulting in a synergistic activation of gene transcription (Fiol et al., 1994). Within the PDE-1 domain, multiple consensus sites for the protein kinases CK II or CK I (see Figure 3A) are found in an arrangement reminiscent of hierarchical phosphorylation sites (Kuenzel & Krebs 1985; Roach 1991). Synthetic peptides encompassing the PDE-1 domain were efficient substrates for CK II, suggesting that phosphorylation at these sites may play an important role in gene regulation (Hai et al., 1989; Foulkes et al., 1991; Smolik et al., 1992; Habener et al., 1995). This domain is also highly conserved among the CREB-related transcription factors ATF-1, CREM, and the Drosophila α-CREB, emphasizing the importance of this site. These observations suggest that a processive phosphorylation cascade initiated by PKA could lead to the sequential phosphorylation of CREB by both GSK-3 and CK II as a mechanism for altering transcriptional activation.

The influence of posttranslational modifications, particularly phosphorylations, on the function of transcription factors has been described in detail (Hunter & Karin 1992; Kwok et al., 1994; Hill & Treisman 1995). The effect of phosphorylation on the regulation of DNA binding has been demonstrated for several transcription factors. Phosphorylation of the POU proteins Oct-1 and Pit-1 by PKA inhibits DNA binding (Kapiloff et al., 1991; Segil et al., 1991). Phosphorylation of the serum response factor (SRF) by CK II potentiates binding to serum response element (SRE) (Manak et al., 1990; Manak & Prywes, 1991) whereas phosphorylation by of c-Myb (Luscher et al., 1990), c-Jun (Lin et al., 1992), Egr-1 (Jain et al., 1996), and Max (Berberich & Cole, 1992) by CK II inhibits binding to their cognate DNA sequences. Phosphorylation at a CamK site (serine 282) of the lymphocyte specific transcription factor ETS1 inhibits binding to the ETS element which is dependent on a sequence of amino acids (QDSFESIESYDSCD) located proximal to the CamK site (Rabault & Ghysdael, 1994). Notably, this site is similar in the triad repeats of serines and acidic residues characteristic of motifs phosphorylated by casein kinases to sequences contained within the PDE-1 domain of the CREB P-box (AESEDSQESVDS). Since CREB has similar phosphorylation motifs as described above, we postulated that a hierarchal phosphorylation cascade initiated by phosphorylation by the primary protein kinase PKA involving phosphorylation of the secondary protein kinases GSK-3 and CKII within the P-box might influence its DNA binding affinity.

The ability of phosphorylation to influence the DNA binding affinities of CREB remains controversial. Some reports have shown that phosphorylation of CREB by PKA results in an increase in binding affinity, especially on low-affinity asymmetric binding sites that deviate from the canonical symmetric site, TGACGTCA (Merino et al., 1989; Weih et al., 1990; Nichols et al., 1992), whereas others reported that phosphorylation of CREB has no effect on its DNA binding affinities (Hagiwara et al., 1993; Richards et al., 1996). Here, we report evidence that PKA and the processive kinase GSK-3 phosphorylate sites within the P-box, thereby altering the DNA binding affinities of CREB.

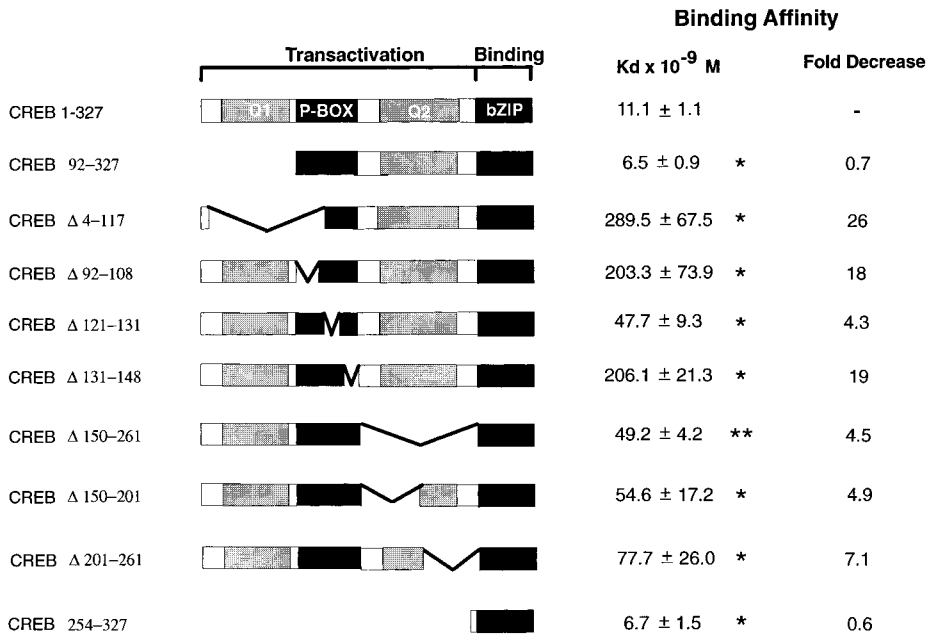

FIGURE 2: Binding affinities of wild-type and mutant CREB for the SMS-CRE. Wild-type CREB (CREB 1−327) is schematically shown with the transactivation and binding domain designated. The transactivation domain contains two glutamine rich regions, Q1 and Q2 (shaded boxes), and the phosphorylation domain, P-box (black box) while the binding domain contains a basic region and leucine zipper, bZIP (black box). The dark lines forming a downward pointing V represent the amino acids which have been deleted. The corresponding dissociation constants (nM) are shown ± the standard error of the mean. Statistical significance compared to CREB 1−327 were calculated from a Student's *t*-test is indicated; one asterisk (*) = $p < 0.05$, two asterisks (**) = $p < 0.005$.

To investigate the effects of phosphorylation on DNA binding, we used a fluorescent electrophoretic mobility shift assay which allows for the determination of the relative binding affinities of CREB to oligonucleotides containing CREs. We show, using in vitro binding assays with recombinant CREB, that sequences within the transactivation domain of CREB, especially those within the P-box influence the binding to a canonical CRE as is contained within the somatostatin promoter (SMS-CRE). Phosphorylation at serine 119 by PKA enhances the binding of CREB to both the symmetric SMS-CRE and the asymmetric CRE located within the somatostatin upstream element (SMS-UE), whereas phosphorylation by GSK-3 at serine 115 attenuates the enhanced binding of CREB mediated by PKA phosphorylation on both elements. Two models of how phosphorylation could effect the activity of CREB and other transcription factors have been proposed: allosteric changes in conformation (Yamamoto et al., 1990; Gonzalez et al., 1991; Brindle et al., 1993; Lee & Masson, 1993) and increases in net surface charge (Parker et al., 1996; Richards et al., 1996). In this report we show that phosphorylation by PKA and GSK-3 alter both the spherical shape and the net surface charge of the CREB/DNA complex. These findings imply that in addition to the regulation of transactivation, a second consequence of the phosphorylation of CREB by PKA in the pathway of cAMP-activated transcription is the regulation of the DNA binding affinity of CREB to CRE promoter elements by altering the structure and charge characteristics of the CREB/DNA complex.

MATERIALS AND METHODS

In Vitro Phosphorylations. Recombinant CREB (pET-CREB) was produced by subcloning CREB cDNA into the bacterial expression plasmid, pET3B, as previously described (Hoeffler et al., 1991). Mutations of CREB were made by utilizing convenient restriction sites or by PCR (polymerase chain reaction)-based mutagenesis and cassette-cloned into wild-type pET-CREB. All manipulations were performed by using established techniques (Sambrook et al., 1989), and mutations were confirmed by DNA sequence analysis (Sanger et al., 1977). After transforming into BL21 (DE3) pLys S bacterial cells, the cells were grown to mid-log phase at 37 °C and induced with 1 μM isopropyl-β-D-thiogalactopyranoside (IPTG, Boehringer Mannheim Corp., Indianapolis, IN) for 3 h. Recombinant CREB was partially purified from the bacterial lysate by resuspending the pellet in Dignams Buffer D (20 mM HEPES, 100 mM KCL, 0.2 mM EDTA, 20% glycerol, and 1 mM PMSF, pH. 7.9), sonicating for 1 min and boiling for 10 min. Following centrifugation (12000*g*), the supernatant containing CREB was removed from the insoluble pellet and stored at −20 °C. The quality of CREB and mutants were assessed by running aliquots on SDS−PAGE and staining with Coomassie blue, which in all cases represented greater than 95% of the total bacterial protein. BSA (bovine serum albumin) standards of known concentrations were run on the same gel to quantitate the amount of CREB and mutants. CREB and mutants were diluted to working concentrations by addition of buffer D containing BSA (1 mg/mL).

Kinase reactions were performed by diluting recombinant CREB to 1 μM in 40 mM Tris-HCl, pH 7.5, 20 mM $MgCl_2$, 1 mM NaF, and 20 μM ATP. Purified protein kinase A (Sigma Chemical Co, St. Louis, MO) at 5 units, purified GSK-3 (New England Biolabs, Inc., Beverly, MA.) at 5 units or purified casein kinase II (New England Biolabs, Inc., Beverly, MA.) at 500 units per 100 pmol CREB was added and incubated for 1 h at 37 °C. The reactions were terminated by incubating at 65 °C for 10 min. To assess phosphorylation efficiency, a 20 μL aliquot was added to 1 pmol of [γ-^{32}P]ATP (6000 Ci/mol, New England Nuclear,

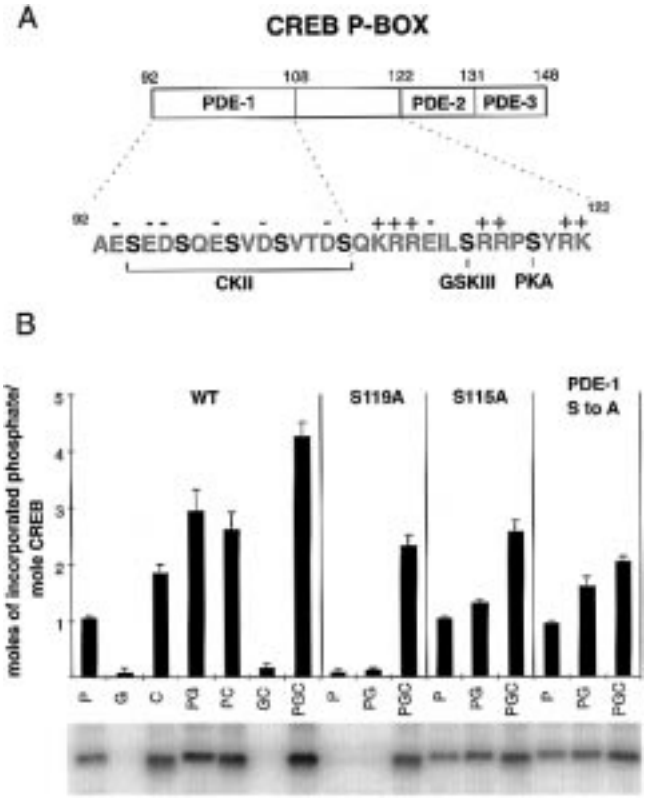

FIGURE 3: PKA and GSK-3 but not CK II processively phosphorylates CREB in vitro. (A) A schematic of the P-box (amino acids 92−148) which is divided into three separates domains PDE-1 (92−108), PDE-2 (122−131) and PDE- 3 (132−148). Amino acids 92−122, which encompasses PDE-1 and both the GSK-3 and PKA sites, are shown. The serines (consensus phosphorylation sites) are highlighted in black and the acidic (−) and basic amino acids (+) are indicated. (B) Wild-type or mutant CREB was phosphorylated as described with either PKA (P), GSK-3 (G), CK II (C), PKA and GSK-3 (PG), PKA and CK II (PC), GSK-3 and CK II (GC), or all three (PGC). The degree of phosphorylation was assessed either by the incorporation of ^{32}P captured on a phosphocellulose filter and counted on a scintillation counter (histogram) or run on SDS−PAGE (autoradiogram) and analyzed on a phosphoimager. The amount of incorporated phosphate was calculated per mole of CREB.

Boston, MA) and the percent incorporation was determined by spotting 5 μL onto phosphocellulose paper, washing with 75 mM phosphoric acid and counting on in a liquid scintillation counter. All phosphorylation reactions were calculated to be greater than 98% complete. Phosphorylation was also assessed to be nearly complete by the degree in which the electrophoretic mobility of CREB is retarded in a nondenaturing gel (see Discussion).

Fluorescent Binding Assays. Oligonucleotides corresponding to the SMS-CRE CCTCCTTGGCTGACGTCAGAGAGAGAGT and ACTCTCTCTCTGACGTCAGCCAAGGAGG, the SMS-UE CGAGGCTAATGTGCGTAAAAGCACTGGT, and ACCAGTGCTTTTACGCACATTAGCCTCG or to Col 8 GATCCGGCTGACGTCATCAAGCTA and TAGCTTGATGACGTCAGCCGGATC were coupled on the 5′ end during synthesis with an fluorescent-phosphoamidite (6-FAM, Perkin-Elmer Applied Biosystems, Foster City, CA). To produce the specific DNA probes, equimolar amounts of each oligonucleotide were annealed by boiling for 5 min and cooled slowly to room temperature. The concentration of the double-stranded oligonucleotide was determined spectrophotometrically by measuring the optical density at A_{260} and multiplying by the extinction coefficient unique for each oligonucleotide as determined by the Oligo 4 analysis program (National Biosciences, Inc., Plymouth, MN), 2.66, 2.74, and 3.15 nmol/OD, respectively.

Fluorescent gel shift assays were performed by incubating 1 pmol of CREB with various amounts of fluorescent probe, typically 2.5 pmol, in a 50 μL reaction containing 10 mM HEPES, 50 mM KCl, 20 mM potassium phosphate, pH 7.9, 0.1 mM EDTA, 10 mM DTT, 0.6 mg/mL BSA, and 10% glycerol at 65 °C for 5 min, to optimize dimer formation, followed by an incubation at room temperature for an additional 30 min. The binding reactions were then loaded on a 6% (19:1 acrylamide:bis acrylamide) nondenaturing polyacrylamide gel and run in a 0.5× TBE buffer (44.5 mM Tris-borate, 44.5 mM boric acid, and 1 mM EDTA) at 180 V. Following electrophoresis, the gel was scanned on the Molecular Dynamics 575 FluorImager with a 530 DF cutoff filter and a PMT voltage of 700. To determine equilibrium binding constants (K_d), the fluorescent probe was titered with a fixed amount of CREB (1 pmol), and the bound and free probe concentrations were quantitated using the Diversity Database analysis software (PDI, Inc., Huntington Station, NY) and applied to Scatchard analysis (Scatchard, 1949) using Excel 5.0 (Microsoft Corp., Redman, WA) to perform the least-squares linear regression analysis. The signal quantitation of the FluoroImager for these probe was linear over the range of 200 to 0.1 pmol. The concentration of bound probe was calculated as (bound/bound + free) × input probe concentration. Free probe concentration was calculated similarly, (free/bound + free) × input probe concentration. All values are shown ± the standard error of the mean. Statistical significance was determined using the Students *t*-Test with one tailed distribution and two-sample unequal variance. The Hill coefficients were calculated by extrapolation from plots of the logs of fractional occupancy of CREB, log[bound CREB/(total CREB − bound CREB)], vs free probe concentrations (Hill, 1910; Cornish-Bowden & Koshland, 1975).

Double filter binding assay was performed as described (Wong & Lohman 1993). Briefly, the nitrocellulose filter (BA83, Schleicher & Schuell, Inc., Keene, NH) was washed in 0.5 M KOH for 5 min, rinsed until neutral pH with MilliQ dH_2O and soaked for 1 h in binding buffer (10 mM HEPES, 20 mM potassium phosphate, pH 7.9, 0.1 mM EDTA, 10 mM DTT, and 10% glycerol). The DEAE filter (NA45, Schleicher & Schuell, Inc., Keene, NH) was washed once in 0.1 M EDTA, pH 8.0, and three times in 1.0 M NaCl for 10 min followed by a quick rinse in 0.5 M NaOH and rinsed with MilliQ dH_2O until neutral pH is obtained. Both filters were placed in a 72 well slot blot apparatus (Schleicher & Schuell, Inc., Keene, NH) with the nitrocellulose filter above the DEAE filter. To determine the association kinetics, a 180 μL binding reaction (as above), lacking the CREB lysate, was mixed and 20 μL filtered as the zero time point. A total of 8 pmol of CREB lysate was then added at room temperature and at the designated time points 25 μL were filtered. To determine the dissociation rate, a 180 μL binding reaction (as above) was mixed and incubated for 30 min at room temperature. A 100-fold excess concentration of unlabeled Col 8 oligonucleotide was added as a high-affinity trap for free CREB, and at the designated time points, 20

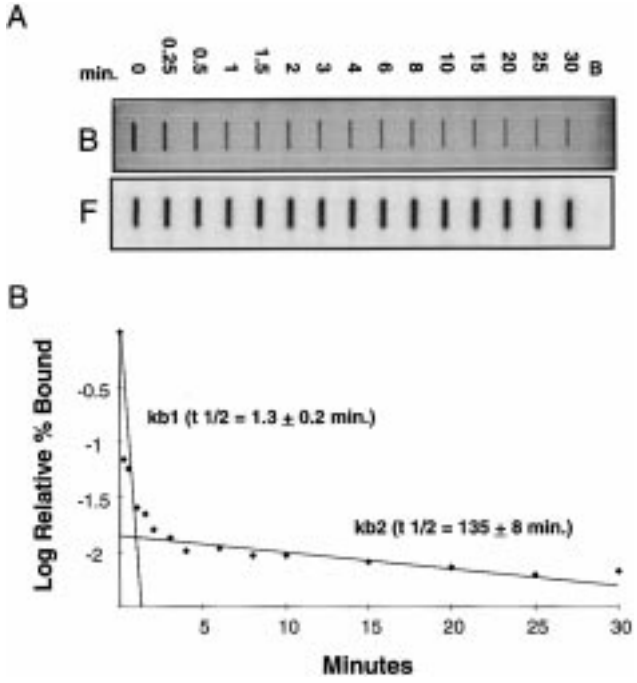

FIGURE 4: Off-rate assay of CREB binding to the F-SMS-CRE. (A) Double-filter binding assay. A total of 10 pmol of CREB lysate is incubated with 5 pmol of F-SMS-CRE in a 20 μL binding reaction for 30 min. A 100-fold excess of unlabeled Col8 is added, and at the designated time points, aliquots are simultaneously filtered through both nitrocellulose, to retain the bound fraction (B), and DEAE which traps the free probe (F). (B) The plot of the log of relative % bound vs time (min) shows a biphasic dissociation response with a fast dissociation rate (K_{b1}) and a slow dissociation rate (k_{b2}). The extrapolated lines used to determine the dissociation rates are shown (solid lines).

μL aliquots were filtered. The binding reactions were filtered by applying a slight vacuum, flow rate of approximately 1 mL/min, and washed with 0.5 mL of binding buffer. The filters were scanned on the FluorImager, face down, as described above. The concentration of bound (C_D) probe was calculated as above. The association rate constant (k_a) was calculated from the following formula, $\ln(C_t - C_D) = kt$, where C_t = total CREB concentration, C_D = bound probe concentration and t = time. $k_a = k/D_t$ where D_t is the total oligonucleotide concentration (Stone et al., 1991). The dissociation rate constant (k_b) was calculated from the following formula, $\ln C_D/C_{D0} = -k_b t$, where C_D is the relative bound probe concentration, C_{D0} = relative bound probe concentration at time zero, and t = time (Riggs et al., 1970; Stone et al., 1991). In all off-rate experiments, the relative bound levels were adjusted to 1 at time zero. The ratio of the free probe was used as a loading control in all of the off-rate assays.

Ferguson Plot Analysis. To determine electrophoretic mobilities (R_f), the binding reactions were run on nondenaturing discontinuous gels. The separating gel was composed of a range of 5 to 9% acrylamide [19:1 acrylamide: bis-(acrylamide)] in 187.5 mM Tris-HCl, pH 8.8. The stacker gel consisted of 4% acrylamide [19:1 acrylamide: bis(acrylamide)] in 62.5 mM Tris-HCl, pH 6.8. The binding reaction solutions were loaded on the gels as described above and were subjected to electrophoresis at 200 V in a 12.5 mM Tris-HCl, 96 mM glycine buffer. Protein standards, with known radii in millimicrons (mμ) (Rodbard & Chrambach 1971; Chrambach 1985), were electrophoresed as controls for size determinations: albumin monomer (2.69 mμ), albumin dimer (3.4 mμ), carbonic anhydrase (2.09 mμ), pepsin dimer (2.75 mμ), ovalbumin monomer (2.34 mμ), ovalbumin dimer (2.94 mμ), β-amylase monomer (3.54 mμ), β-amylase dimer (4.46 mμ), and β-amylase trimer (5.11 mμ). After scanning the gels on the FluorImager, the migration distances (R_f) were measured using the Diversity Database analysis software (PDI, Inc., Huntington Station, NY).

To obtain slopes (K_r) and y-intercepts (Y_o), the R_f values were analyzed by the RFT1 analysis program which calculates an unweighted least-squares linear regression line from the plot of the log R_f vs percent acrylamide. These results were then compared to a weighted regression line, maximum likelihood method with 10 iterations, and differences were designated as the standard deviation of the experiment. The radii of the CREB/DNA complexes were analyzed on the GIANTRUN analysis program which calculates an unweighted least-squares linear regression line from the plot of the square root of Kr vs radii. The correlation coefficient from the line derived from the standard curve reported in Figure 5F was 0.934. The valence was calculated by applying the derived Y_o and radius values to the CHARGE analysis program. The RT/f, GIANTRUN, and CHARGE analysis programs were developed by David Rodbard and Loel Graber at the National Institute of Child and Human Development, Reproduction Research Branch, National Institutes of Health, Bethesda, MD (Rodbard and Chrambach 1971; Chrambach 1985).

RESULTS

Fluorescent Gel Shift Assay Measurements of the Binding Affinity of CREB to a cAMP Response Element. The electrophoretic mobility shift assay is a well established method for determining the relative affinities of many DNA binding proteins for their cognate DNA recognition sequences (Baker et al., 1986; Stone et al., 1991; Anderson & Dynan, 1994). To more accurately determine the binding affinity of CREB for its cognate DNA elements, a fluorescent gel shift assay was developed. Two complementary oligonucleotides, corresponding to the high-affinity CRE located within the promoter of the rat somatostatin gene (see Materials and Methods), were synthesized with fluorescein attached to the 3′ ends and were annealed to produce a double stranded DNA probe (F-SMS-CRE). To assay for DNA binding affinities, the fluorescent oligonucleotide probe was titered and incubated with a fixed amount (1 pmol) of recombinant CREB using standard binding conditions (Fried & Crothers, 1981; Baker et al., 1986; Stone et al., 1991). The bound and free probes were resolved on nondenaturing polyacrylamide gels, scanned with a fluorimager (Molecular Dynamics FluorImager 575) and quantitated by image analysis software. A representative gel is shown in Figure 1A. To examine whether the running conditions altered the binding kinetics, an experiment was done by which CREB bound to the F-SMS-CRE was run on a denaturing electrophoresis gel and at 15 min intervals the gel was removed, scanned, and the bound/free ratio quantitated. As shown in Figure 1E, the bound/free ratio changed negligibly during the 1.5 h run, with either phosphorylated or unphosphorylated CREB. These results further support the validity of this

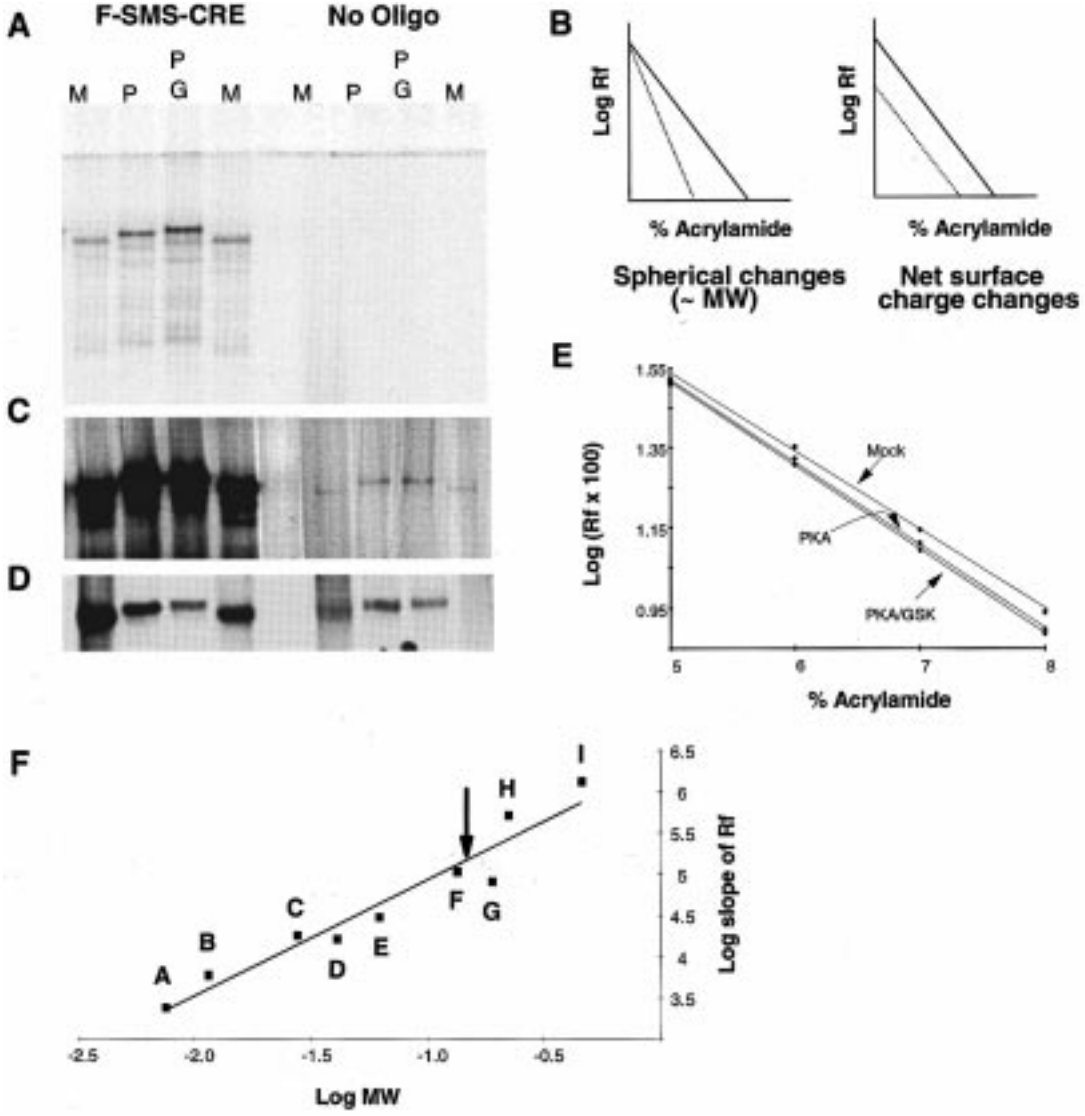

FIGURE 5: Phosphorylation of CREB alters the migration through a nondenaturing electrophoresis gel. (A) CREB binding to the F-SMS-CRE on a nondenaturing discontinuous gel. CREB (5 pmol) was either mock phosphorylated (M), phosphorylated with PKA (P), or phosphorylated with both PKA and GSK-3 (PG), incubated in a standard binding reaction with either fluorescent oligonucleotide containing the SMS-CRE (left) or no DNA (right) and run on a discontinuous nondenaturing gel. The scan from the FluorImager is shown. (B) Ferguson plot theory. Plotting the log of migration distance (log R_f) vs acrylamide concentration produces a straight line (—). A retardation in migration due to phosphorylation either alters the slope or *y*-intercept of the line (···). An increase in the slope indicates an increase in spherical size (which correlates to an increase in molecular weight) while a parallel decrease in *y*-intercept indicates an increase in positive net charge. (C) The same gel as shown in Figure 5A was soaked in a solution containing a fluorescent oligonucleotide encoding a high-affinity CRE (Col 8) and was rescanned after washing away the free probe. (D) An immunoblot in which a similar gel was probed with a CREB specific antibody using chemiluminescence for detection. (E) Results from the Ferguson plot analysis of phosphorylated CREB binding to the SMS-CRE. CREB was phosphorylated as above, incubated in a standard binding reaction with a fluorescent oligo containing the SMS-CRE and run on discontinuous nondenaturing gels containing various percentages of acrylamide. The average migration distances from six independent experiments were determined and the log of these distances (log R_f x 100) was plotted against percent acrylamide concentration. Arrows designate which line corresponds to the phosphorylated state of the CREB/DNA complex. The standard errors of the mean and are as follows for 5, 6, 7, and 8% acrylamide, respectively, Mock (0.0054, 0.0107, 0.0133, and 0.0100), PKA (0.0065, 0.0107, 0.0141, and 0.0119), and PKA/GSK (0.0072, 0.0112, 0.0137, and 0.0068). (F) Determination of the molecular weight of the CREB/F-SMS-CRE complex by plotting the log slopes (K_r) calculated from Ferguson plots of known protein standards versus the log molecular weights from four independent experiments. The protein standards are shown: A, carbonic anhydrase (29 kDa); B, ovalbumin monomer (43.5 kDa); C, pepsin dimer (71 kDa); D, albumin monomer (68 kDa); E, ovalbumin dimer (87 kDa); F, β-amylase monomer (152 kDa); G, albumin dimer (136 kDa); H, β-amylase dimer (304 kDa); and I, β-amylase trimer (456 kDa). The correlation coefficient derived from this line is 0.934. The arrow shows the predicted size of the prominent CREB/F-SMS-CRE complex (172 ± 13 kDa).

fluorescent gel shift assay in the determination of binding affinities.

The binding of CREB to the F-SMS-CRE exhibits a typical saturation curve (Figure 1B) with a sigmoidal curve observed at lower concentrations, suggesting that a cooperative interaction occurs between CREB and the F-SMS-CRE (see insert in Figure 1B). The Hill plot (Figure 1C) reveals that CREB binds to the F-SMS-CRE with both positive and negative cooperativity (Cornish-Bowden and Koshland, 1975). The Hill coefficients, calculated from the extrapolated lines (solid lines in Figure 1C) of three independent experiments, are 2.06 ± 0.19 and 0.374 ± 0.087 in support of

dual cooperativity. The nonlinear Scatchard plot also supports the observations from the Hill plot analysis, that cooperative binding events are occurring (broken line Figure 4D). To simplify the analysis of the effects of phosphorylation and the mutations of CREB on DNA binding, the dissociation constants were determined only for the high-affinity binding interactions as defined from the values which lie on the upper end of the saturation curve and are linear on the Scatchard plot. Within this region of the saturation curve, we can confidently apply bimolecular kinetic analysis. Linear regression analysis of the line derived from the Scatchard plot of the values shown in Figure 1B (solid line Figure 1D) shows that CREB binds the SMS-CRE with a dissociation constant of 11.1 ± 1.1 nM, a value within the range of those reported previously for the binding of CREB to CREs (Hagiwara et al., 1993; Williams et al., 1993; Anderson and Dynan, 1994; Richards et al., 1996; Yin & Gaynor, 1996). However, the Hill plot and nonlinear Scatchard analysis indicate that the binding of CREB is more complex than can be explained by a simple bimolecular interaction and that other binding interactions between CREB and DNA occur. Because of the high degree of accuracy that can be obtained in determining the concentrations of the fluorescent oligonucleotide probes, the fluorescent gel shift assay appears to provide a reliable method for the accurate analysis of CREB on DNA binding.

Sequences within the Transactivation Domain of CREB Are Required for High-Affinity DNA-Binding. To define the regions of CREB that are important in regulating DNA binding, a series of deletion mutations were constructed in the CREB cDNA and the resulting bacterially expressed proteins were analyzed utilizing the fluorescent gel shift assay with the F-SMS-CRE probe (Figure 2). With all the mutants, a complex kinetic profile similar to the wild-type CREB was demonstrated; thus, only the high-affinity interaction was assessed. CREB lacking the N-terminal Q1 region but containing an intact P-box (CREB 92−327) bound with a slightly higher affinity (K_d = 6.5 ± 0.9 nM) than wild-type CREB (K_d = 11.1 ± 1.1 nM), suggesting that a DNA binding destabilization region lies within the amino-terminal (Q1) region of CREB. When the amino acids located N-terminal to the P-box (containing the Q1 region) and half of the P-box including PDE-1, the GSK-3 and the two basic residues (RR) of PKA phosphorylation were deleted (CREBΔ 4−117) and a marked 26-fold reduction in binding affinity was observed. These findings imply that sequences within the P-box contribute to the higher affinity binding of CREB to the CRE. Block deletions of amino acids within the P-box were tested to define further the regions responsible for the high-affinity binding. The removal of the PDE-1 (CREB Δ92−108) and PDE-3 (CREB Δ 131−141) domains caused a dramatic reduction in binding affinity, approximately 18-fold for both deletions, whereas deletion of the PDE-2 domain (CREB Δ121−131) caused only a slight decrease in binding affinity of 4-fold (Figure 2). The effects of deleting amino acid sequences between the P-box and bZIP domain on DNA binding were also examined. Removal of the regions between the P-box and the bZIP domain, including the Q2 region, (Δ150−261, Δ150−201, and Δ201−261) also resulted in a small but significant reduction in binding affinity, 4-, 5-, and 7-fold, respectively. Notably, the affinity of binding of the somatostatin CRE to the bZIP region of CREB alone (CREB Δ254−327) was approximately 2-fold higher than is observed for the wild-type CREB. These findings indicate that amino acid sequences located within the P-box promote a higher affinity binding of CREB to the F-SMS-CRE and may be important in the regulation of the transcriptional activity of CREB in vivo. Furthermore, the N-terminal Q1 domain (aa 1−92) may act as a binding destabilization region that is influenced by the amino acids within the P-box.

Hierarchal Phosphorylation within the P-Box of CREB Takes Place between the Protein Kinases PKA and GSK-3 but Not CK II. Deletion of the PDE-1 domain within the P-box of CREB resulted in a marked reduction of the binding affinity for the SMS-CRE (CREBΔ 92−108 in Figure 2). The PDE-1 region is of interest because it lies N-terminal to the sites phosphorylated by PKA (serine 119) and GSK-3 (serine 115), and also contains consensus sites for phosphorylations by CKII (serine 94, 97, 100, 103, 107) in an arrangement reminiscent of hierarchal phosphorylation (Figure 3A) (Fiol et al., 1990; Roach 1991). Also of interest, the PDE-1 domain contains several negatively charged amino acids interspersed with serines (aa 93−106). In view of the results from the deletion mutations, we propose that alterations in the amino acids within the PDE-1 domain due to phosphorylation may play an important role in the regulating of the DNA binding properties of CREB. To test whether CREB is a substrate for hierarchal phosphorylations by PKA, GSK-3, and CKII, equal amounts of CREB-327 was phosphorylated in vitro using individual kinases and the total reaction mix was either analyzed on phosphocellulose paper and counted in a scintillation counter (histogram shown in Figure 3B) or resolved by SDS−PAGE and analyzed on a Phosphoimager (shown on lower part of Figure 3B). Since we were concerned that each kinase may alter the activity of each other, which has been demonstrated for GSK-3 altering the activity of PKA (Hemmings et al., 1982), we sequentially added each kinase after inactivation of the initial kinase by boiling. As expected, CREB is an efficient substrate for PKA with mol of phosphate incorporated for every mole of CREB (Figure 3B). Substitution of serine 119 with alanine (S119A) abolishes the phosphorylation of CREB by PKA, confirming the known high specificity of PKA for serine 119. CREB is not phosphorylated by GSK-3 alone, but is a potent substrate when CREB is first phosphorylated by PKA, confirming previous reports that GSK-3 acts as a processive kinase on CREB once phosphorylated by PKA (Fiol et al., 1994). Unexpectedly, the molar incorporation of [^{32}P]ATP by GSK-3 on PKA-phosphorylated CREB is twice that of anticipated, indicating that GSK-3 processively phosphorylates another site in addition to serine 115. Substitution of serine 115 with alanine abolished the phosphorylation of CREB by GSK-3. CKII phosphorylates each mole of CREB with 2 mol of phosphate, and the levels are additive after phosphorylation by PKA alone or in combined treatment with GSK-3 with a total of 4 or 5 mol of phosphate/CREB when treated with all three kinases (Figure 3B). Interestingly, wild-type CREB was consistently not phosphorylated by the combined addition of GSK-3 and CK II, of which we can provide no explanation. Substitution of the five serines in the PDE-1 domain for alanines (PDE-1 S to A) attenuated the phosphorylation of CREB by CKII. These results indicate that CREB is phosphorylated by CKII at two

Table 1: Equilibrium Binding Affinities of Phosphorylated CREB to the SMS-CRE and SMS-UE[a]

	SMS-CRE		SMS-UE	
	k_d (nM) ± SE	*n*	k_d (nM) ± SE	*n*
Mock	15.8 ± 2.7	7	180 ± 41	5
PKA	4.9 ± 1.4[b]	7	72 ± 17[c]	5
PKA/GSK	13.8 ± 3.3	4	147 ± 26	5
PKA/GSK/CK	9.7 ± 0.7	4	ND[d]	

[a] Results from Scatchard analysis of the fluorescent gel shift assay of mock, PKA, PKA/GSK-3, or PKA/GSK-3/CK II phosphorylated CREB. The equilibrium dissociation constants are shown (K_d) in nanomolar ± the standard error of the mean. The number of experiments are indicated (*n*). Statistical significance has been calculated from a Student's *t*-Test. [b] $p < 0.005$. [c] $p < 0.05$. [d] ND = not determined.

Table 2: Dissociation Binding Affinity of Phosphorylated CREB to the SMS-UE[a]

	off rate k_{b2} (min^{-1}) ± SE	$t_{1/2}$ (min)	calcd K_d (k_{b2}/k_a (nM)	*n*
Mock	0.0130 ± 0.0025	53.4	150	7
PKA	0.072 ± 0.0019[b]	95.9	83	7
PKA/GSK	0.0105 ± 0.0024	65.9	121	6

[a] Results from the kinetic double filter assay of mock, PKA, or PKA/GSK-3 phosphorylated CREB. The off-rates (k_{b2}) are shown ± the standard error of the mean. The half-life ($t_{1/2}$) is also shown. The calculated equilibrium binding constants (K_d) are derived from dividing the dissociation constants (k_{b2}) by the association constant (k_a) as described in the text. The number of experiments are indicated (*n*). Statistical significance was calculated from a Student's *t*-Test. [b] $p < 0.05$.

sites within the PDE-1 domain; however, phosphorylation by CKII appears not to be involved in the hierarchal phosphorylation cascade within the CREB P-box involving PKA and GSK-3. The processive phosphorylation of the CREB PDE-1 S to A mutation by PKA and GSK-3 was reduced by 1 mol of phosphate, indicating that the second GSK-3 phosphorylation site is located within the PDE-1 domain. All together, these results indicate that PKA and GSK-3, but not CKII, are involved in the processive phosphorylation of CREB within the P-box and all three kinases may participate in altering the DNA binding affinities of CREB.

Phosphorylation of CREB by PKA and GSK-3 Alters DNA Binding Affinities of CREB. To determine whether the phosphorylation of CREB by processive kinases, PKA and GSK-3, affects DNA binding affinities, CREB was phosphorylated in vitro with the kinases and binding to the F-SMS-CRE was assayed by the fluorescent gel shift assay (Table 1). Since CK II was not implicated in the processive phosphorylation cascade of CREB and had little effect on the binding affinity alone (data not shown) or in combination with PKA and GSK-3 (Table 1), we chose not to further investigate its influence on DNA binding activity. Phosphorylation by PKA resulted in a 3-fold increase in binding affinity for the SMS-CRE. It is not clear why the mock phosphorylation reaction resulted in a decrease in a binding affinity of CREB (11.1 ± 1.1, Figure 2, to 15.8 ± 2.7, Table 1); however, the increase in binding affinity in response to phosphorylation by PKA was consistently observed in all experiments. Surprisingly, the secondary phosphorylation by GSK-3 reversed the enhanced DNA binding mediated by PKA, suggesting that phosphorylation by GSK-3 attenuates the increase in DNA binding induced by phosphorylation by PKA. Because other workers have reported an increase in the binding of CREB to nonsymmetrical CREs by PKA-mediated phosphorylation (Nichols et al., 1992), we examined whether phosphorylation by PKA and GSK-3 may alter its binding affinity to the asymmetric CRE located within the somatostatin upstream enhancer element (SMS-UE) of the somatostatin promoter (Vallejo et al., 1992a,b). As shown in Table 1, CREB binds to the SMS-UE with approximately a 10-fold lower affinity than to the symmetrical SMS-CRE. The effect of phosphorylation of CREB on the affinity of its binding to the SMS-UE was similar to that of its binding to the SMS-CRE, a 2.5-fold increase in binding affinity in response to phosphorylation by PKA followed by an attenuation in binding due to the subsequent phosphorylation by GSK-3. These results indicate that the phosphorylation of CREB by PKA results in an increase in DNA binding affinity on both high (F-SMS-CRE)- and low (F-SMS-UE)-affinity CREs. Furthermore, a secondary phosphorylation of CREB by GSK-3 inhibits DNA binding to both the high- and low-affinity CREs.

Because the validity of electrophoretic mobility shift assays for determinations of the equilibrium dissociation constants for CREB has been questioned (Lundblad et al., 1996; Richards et al., 1996), we confirmed the effects of PKA and GSK-3 phosphorylation on the binding affinities of CREB by utilizing an alternative method. A kinetic approach utilizing a double filter binding assay was chosen for determining both the rates of association and dissociation (Riggs et al., 1970; Hinkle & Chamberlin, 1972; Wong and Lohman, 1993). The dissociation (off) rates were determined by incubating CREB with fluorescently labeled SMS-CRE for 30 min in standard binding reaction. A 100-fold excess of unlabeled oligonucleotide corresponding to the high-affinity Col 8 binding site was then added as a competitive trap for free CREB and at various time points an aliquot was filtered through nitrocellulose (Figure 4). The nitrocellulose retains the bound CREB/DNA complex (Figure 4A, assay B), whereas the free probe was captured on a DEAE filter, which was placed beneath the nitrocellulose filter (Figure 4A, assay F). After washing, both filters were scanned, face down, on the FluorImager, and the ratios of the bound and free probe were quantitated. As shown in Figure 4B, the dissociation assay reveals that CREB binds to the F-SMS-CRE with biphasic kinetics, a fast low-affinity interaction (K_{b1}, $t_{1/2} = 1.3 \pm 0.2$ min) and a slower high-affinity interaction (k_{b2}, $t_{1/2} = 135 \pm 8$ min). These results showing biphasic dissociation kinetics further support the equilibrium data indicating that multiple interactions are involved in the binding of CREB with the F-SMS-CRE.

Since the high-affinity off-rate (K_{b1}) for the binding of CREB to the F-SMS-CRE was extremely long and therefore difficult to reproducibly quantitate accurate off-rates, changes due to phosphorylation were difficult to detect. We, therefore, chose to test the effects of phosphorylation on the binding of CREB to the F-SMS-UE, which has a faster off-rate (Table 2). Using the double filter binding assay as described above, we determined both the association and the dissociation kinetics for the binding of CREB to the F-SMS-UE. The off-rate assay showed a similar biphasic response, a low affinity (K_{b1}) and a high-affinity (k_{b2}) interaction, with $t_{1/2}$ off-rates of 0.404 ± 0.028 min and 53.4 ± 10.2 min, respectively. The reduced $t_{1/2}$ for the slow dissociation rate

(k_{b2}) and fast dissociation rates (k_{2a}) as compared with those determine for the F-SMS-CRE is consistent with the SMS-UE being a lower affinity binding site for CREB. The affect of phosphorylation by PKA caused a significant decrease in the slow high-affinity rates (k_{b2}) (Table 2), whereas the processive phosphorylation by GSK-3 attenuated this response consistent with the data obtained from the equilibrium binding studies (Table 1). Interestingly, there was no significant effect by phosphorylation on the fast low affinity rates (data not shown). The association rates (k_a) for the F-SMS-UE was calculated to be $86\,500 \pm 14\,000$ M^{-1} min^{-1} and was also not shown to change significantly due to the phosphorylation state. As shown in Table 2, the calculated dissociation constants (k_{b2}/k_a) from the kinetic assays (Stone et al., 1991) are in good agreement with the values determined from the equilibrium experiments (Table 1). Collectively these observations indicate that the phosphorylation of CREB by PKA results in a significant increase in binding affinity for both the SMS-CRE and SMS-UE and the affinities are attenuated by the processive phosphorylation of CREB by GSK-3.

Phosphorylation of CREB by PKA and GSK-3 Alters Its Spherical Shape and Net Surface Charge. Analyses of the gel shift experiments indicated that phosphorylation of CREB by PKA and GSK-3 affected the electrophoretic mobilities of the CREB/DNA complexes (Figure 5A). We sought to take advantage of these altered electrophoretic mobilities to address questions about how phosphorylation can alter the structural characteristics of CREB using Ferguson plot analyses (Ferguson 1964; Rodbard and Chrambach, 1971; Chrambach, 1985). Ferguson plot analyses depend on the premise that the two major factors influencing the electrophoretic migration of a molecule through nondenaturing gels are size and net surface charge. As diagrammed in Figure 5B, plotting the log of the migration distance (log R_f) vs acrylamide concentration yields a straight line (solid line). If two proteins differ only in spherical shape (which correlates to molecular weight), there will be a change in the slope of the lines with a higher slope, indicating an increase in spherical size (broken line). On the other hand, if two molecules differ only in net surface charge, a parallel shift in the lines will occur, as indicated by a change in *y*-intercept, with a downward shift, indicating an increase in positive net surface charge (broken line). Analysis of Ferguson plot data by RTF1, GIANTRUN. and CHARGE computer programs allows for the quantitative determination of the changes in both spherical size and valence (Rodbard & Chrambach, 1971; Chrambach, 1985). When the Ferguson analysis is applied to the CREB/DNA complex, it will allow distinction between the conformational and/or net surface charge changes that occur in response to phosphorylations of CREB.

To improve the resolution of CREB/DNA complexes and to more accurately measure distances of electrophoretic mobilities (R_f), we ran the CREB binding reactions on discontinuous nondenaturing gels, as shown in Figure 5, panels A, C, and D. This biphasic gel system not only improves the resolution of the CREB/DNA complex, but also focuses the free probe to the bottom of the gel, which is used as the end point for the determinations of R_f (the origin is the interface between the stacker and separating gels). As shown in Figure 5A, phosphorylation by PKA causes a decrease in electrophoretic mobility. Phosphorylation by both PKA and GSK-3 causes a further reduction in mobility. To test whether the changes in the mobility of CREB in response to phosphorylation is inherent to CREB itself or is dependent on its binding to DNA, aliquots of CREB phosphorylated by the various protein kinases were also analyzed by gel electrophoresis in the absence of any DNA (Figure 5A, right). After scanning to determine the location of the fluorescently labeled CREB/DNA complex (Figure 5A), the gel was soaked in a solution containing 100 nM of a high-affinity fluorescently labeled oligonucleotide (F-Col8) to act as a CREB-specific stain. As shown in Figure 5C, F-Col8 specifically stained the phosphorylated CREB and the relative mobilities were indistinguishable, either in the presence or absence of DNA. Subsequent experiments have determined that the difference in intensity between the lanes containing the fluorescent probe and the DNA-free lanes shown in Figure 5C is due to the fact that this post-staining procedure with F-Col8 is inefficient. Figure 5D shows an immunoblot prepared from an identical gel using a CREB-specific antiserum, further supporting the findings that the shift in electrophoretic mobilities due to phosphorylation is independent of DNA.

Ferguson plot analysis of multiple gels which contain known protein standards has been successfully utilized to determine the molecular weights of nondenatured proteins, particularly multimeric complexes (Bryan, 1976). Figure 5F shows that the molecular mass of the major bound CREB fragment (see Figures 1A and 5A) as determined by Ferguson plot analysis to be 172 ± 13 kDa. This calculated molecular weight is consistent with CREB existing as a tetramer binding to two oligonucleotides [(37 kDa $\times$ 4) + (15 kDa $\times$ 2)]. An important result from the immunoblot experiments is that most of the CREB that was electrophoresed both in the presence and absence of DNA exists as multimers, since no CREB monomers were detected. These findings indicate that CREB exists predominantly as a tetramer even in the absence of DNA. The concentration of CREB in this experiment is 250 nM, which is nearly one hundred times less than the dimerization constant reported for the CREB bZIP domain alone in the absence of DNA (Santiago-Rivera et al., 1993). These observations suggest that the amino terminal sequences of CREB may facilitate the multimerization of CREB.

The results of the Ferguson plot analysis of CREB phosphorylated by PKA alone and the combined treatment of PKA and GSK-3 are shown in Figure 5E and Table 3 from a single analysis of seven independent experiments. All seven experiments showed consistent and reproducible changes in slope and *y*-intercept upon PKA phosphorylation, an increase in slope along with a shift in the *y*-intercept toward the positive direction. These results indicate that phosphorylation on serine 119 induces a conformational change in the CREB/DNA complex, a 3.1% increase in spherical shape (Table 3), which has a greater mass than predicted from the addition of a single phosphate group. However, since we have no way of knowing the spherical area imposed by a single phosphate group, we cannot be confident that this observed increase in spherical size is due solely to the addition of the phosphate group. PKA phosphorylation also results in an increase in positive net surface charge by the equivalent of 5 protons per CREB/

Table 3: Changes in Spherical Size and Net Surface Charge of Phosphorylated CREB[a]

	K_r (log RF/%A)	Y_o (antilog *y*-int)	r_2	spherical size		valence	
				(mμ)	%Δ	(H^+/mol)	%Δ
Mock	0.190	3.022	0.998	3.862		34.9	
PKA	0.202	3.280	0.998	3.982	3.1	38.7	+4.8
PKA/GSK	0.207	3.415	0.998	4.026	4.2	42.0	+7.2

[a] Results from a Ferguson plot analysis of mock, PKA, or PKA/GSK-3 phosphorylated CREB. The slopes (k_r) and the antilog of the *y*-intercepts (Y_o) were calculated from a weighted linear aggression analysis of a Ferguson plot from seven independent experiments (shown in Figure 5E) by using the RFT1 program. The correlation coefficient (r_2) of these weighted lines are shown. The spherical size in millimicrons (mμ) were calculated from the shown K_r and Y_o values utilizing the GIANTRUN analysis program and the percent differences (%Δ) from mock are shown. The net surface charges (valence) was calculated from the CHARGE analysis program and are quantified as protons per molecule with the difference (Δ) from mock shown.

DNA complex (Table 3). This is an interesting finding, since the addition of a phosphate group would be predicted to decrease the net charge by 2 protons per CREB molecule or 4 protons per CREB dimer in the DNA complex; therefore, the actual gain of positive charges due to phosphorylation by PKA could be as high as 9 protons per CREB/DNA complex. Processive phosphorylation by GSK-3 reproducibly induces a further 1.1% increase in spherical size along with an increase in net surface charge of 2 protons. Since we demonstrated that two phosphates per CREB molecules were added by the processive GSK-3 (Figure 3), the total increase in net surface charge due to the effect of GSK-3 could be as high as 10 additional protons per CREB/DNA complex. These results suggest that phosphorylation within the P-box by PKA and GSK-3 induces a conformational change within CREB resulting in either the exposure of positively charged amino acids or the masking of negatively charged amino acids from the surface. It is not clear what proportion of the total net charge is being altered by phosphorylation, since the conformational changes could mask the negative charges of the phosphate groups or the charged amino acids within CREB. Nonetheless, the changes in conformation and net surface charge of CREB induced by PKA and GSK-3 phosphorylations could alter the DNA binding affinities and transcriptional activity of CREB.

Acidic Amino Acids within the PDE-1 Domain Are Important for Regulating DNA Binding. We have shown that phosphorylation of CREB by PKA induces a conformational change in CREB, resulting in an increase in positive net surface charge along with an increase in DNA binding affinity. GSK-3 causes a further increase in spherical shape and net surface charge, yet attenuates the increase in DNA binding affinity in response to phosphorylation by PKA. We also have shown that the PDE-1 domain, which contains many acidic amino acids, is required for high-affinity binding. Therefore, we tested whether these acidic amino acids are necessary for high affinity binding. Various substitution mutations were designed to alter the net charge of the PDE- 1 domain (Table 4) by either substituting the five serines with neutral alanines (PDE-1 S to A), glutamic acids (PDE-1 S to E), or arginines (PDE-1 S to R) or substituting four of the acidic amino acids with neutral alanines (PDE-1 E/D to A) or arginines (PDE-1 E/D to R). As shown in Table 4, these substitutions would be predicted to alter the net charge within the PDE-1 domain ranging from -11 to $+3$ protons. The equilibrium binding analysis using F-SMS-CRE demonstrated that these charge alterations greatly affected the binding affinities for the SMS-CRE. For instance, a decrease in acidic charge correlates with a decrease in binding affinity; making the PDE-1 domain more acidic (PDE-1 S to E) had little effect on binding, whereas converting the PDE-1 domain to a net basic charge of $+3$ (PDE-1 E/D to R) effectively eliminated binding. This situation suggests that the acidic amino acids within the PDE-1 domain are required for high-affinity binding. The conversion of the serines to alanines resulted in a 5-fold decrease in binding affinity, even though the predicted charge remained the same. One explanation for this result might be that the conversion from hydrophilic serine to hydrophobic alanines could inhibit binding, implicating the importance of hydrophobic interactions as well as ionic interactions. Alternatively, the introduction of alanines may alter the conformation of CREB, i.e., α-helicity, thereby influencing the total net charge of CREB. These results demonstrate that the acidic amino acids within the PDE-1 domain of CREB contribute to high-affinity DNA binding.

To address how these amino acid substitutions that alter DNA binding also alter the spherical shape and net surface charge of CREB, Ferguson plots were constructed and analyzed by the RFT1, GIANTRUN, and CHARGE programs. All the charge change substitutions resulted in an approximate 8% decrease in total spherical size (Table 4). These results suggest that both the serines and acidic amino acids within the PDE-1 domain are responsible for maintaining a wild-type conformation. It is interesting to note that none of the substitutions mimic the effect of phosphorylation by PKA and GSK-3, an increase in spherical size of 3.1 and 4.2%, respectively (Table 3). The most likely explanation for this circumstance is that simultaneous changes of multiple amino acids may disrupt the observed effect of the phosphorylations. However, it does seem clear that the amino acids within the PDE-1 domain are important for maintaining a wild-type conformation.

The effect of these amino acid substitutions on the calculated net surface charge is more dramatic. First, the total change in net charge between the various mutants is less than the predicted charges (Table 4), i.e., PDE-1 E/D to R substitution mutant is predicted to change by $+9$ protons, whereas it is measured to change by only $+5$ protons. At least two possibilities could account for this: (1) not all of the charged amino acids within the PDE-1 domain are exposed to the surface in solution, or (2). these mutation alter the conformation of CREB, thus, either exposing or masking charged amino acids which lie elsewhere in CREB. Second, the calculated net surface charge for two mutations were not as predicted; PDE-1 S to A would be not be predicted to have any change in net charge yet a decrease in 2 protons was observed while the PDE-1 S to E was observed to increase its net surface charge by 2 protons when it was predicted to decrease its charge by 5 protons. These results imply that the charged amino acids which lie outside of the PDE-1 mostly contribute to the net surface charge of CREB in solution, and that the acid amino acids within the PDE-1 domain are responsible for maintaining protein conformation. Finally, the calculated net surface charge of the mutations correlates better with the binding affinity than with the

Table 4: Charged Amino Acids within the PDE-1 Domain of CREB Influence DNA Binding to the SMS-CRE, Spherical Shape and Net Surface Charge[a]

		predicted net charge			calculated spherical size		calculated net surface charge	
		(H^+/mol)	Δ	binding affinity (nM)	(mμ)	%Δ	(H^+/mol)	Δ
PDE-1 WT	AESEDSQESVDSVTDSQ	−6		11.1 ± 1.1	3.86		+34.9	
PDE-1 S to A	AE**A**ED**A**QE**A**VD**A**VTD**A**Q	−6	0	61.5 ± 2.9	3.55	−8.2	+32.8	−2.1
PDE-1 S to E	AE**E**ED**E**QE**E**VD**E**VTD**E**Q	−11	−5	29.0 ± 9.9	3.60	−6.7	+37.0	+2.1
PDE-1 S to R	AE**R**ED**R**QE**R**VD**R**VTD**R**Q	−1	+5	114.2 ± 21.2	3.54	−8.3	+38.3	+3.4
PDE-1 E/D to A	AES**A**DSQ**A**SV**A**SVT**A**SQ	−2	+4	100.5 ± 4.8	3.55	−8.0	+38.5	+3.6
PDE-1 E/D to R	AES**R**DSQ**R**SV**R**SVT**R**SQ	+3	+9	>500	3.54	−8.3	+39.8	+4.9

[a] Sustitution mutations of either serines (S) or acidic amino acids (E/D) are highlighted. The predicted net charge resulting from these mutations are indicated as protons per molecule (H^+/mol) with the differences (Δ) from wild-type (WT) CREB shown. The binding affinities were calculated from fluorescent gel shift assays as described in Figure 1D and shown as dissociation constants (nM) ± the standard error of the mean of three or more experiments. The mutations were analyzed by Ferguson plots (Figure 6) and the spherical shape and net surface charge were calculated as described in Table 3. The spherical shapes in millimicrons (mμ) are shown with the percent differences (%Δ) from wild-type CREB. The net surface charge is indicated as protons per molecule with the differences (Δ) from wild-type CREB shown.

predicted charge changes, i.e., an increase in positive net surface charge results in a decrease in binding affinity. The only exception to this is from the serine to alanine mutation (PDE-1 S to A), which may result in a disruption of the α-helicity of this region, thereby effecting binding to a greater degree than the effect of the altered net surface charge. The results do suggest that charged amino acids within the PDE-1 domain CREB are critical for high-affinity binding to CREs.

DISCUSSION

The phosphorylation of transcription factors in response to the activation of cellular signal transduction pathways is a commonly utilized mechanism for translating extracellular signals to changes in gene expression (Hunter and Karin 1992; Hill and Treisman, 1995). The phosphorylation of transcription factors may exert either positive or negative effects on gene transcription. The molecular mechanisms by which phosphorylations alter the activities of transcription factors are not fully understood. Here, we describe experiments using the cAMP-activated phosphorylation of the transcription factor CREB as a model to address mechanisms by which phosphorylation may alter the binding affinity of CREB to its DNA enhancer element. Because reports describing the effects of the phosphorylation of CREB on its DNA binding functions have been in disagreement (Merino et al., 1989; Weih et al., 1990; Nichols et al., 1992; Hagiwara et al., 1993; Richards et al., 1996), we initiated a detailed analysis of the effects of phosphorylations on the binding activities of CREB, using a newly devised, sensitive fluorescent gel shift assay. By titering the amounts of fluorescently tagged oligonucleotide containing a binding site for CREB in the presence of a fixed concentration of CREB and accurately measuring the concentration of the bound and free complexes, we determined the high-affinity dissociation constants for the binding of CREB to its cAMP response element (CRE).

Analyses of the binding of CREB to the fluorescently labeled somatostatin CRE (F-SMS-CRE) revealed that the binding is not a simple bimolecular interaction. The sigmoidal saturation curve describing the kinetics of the binding of CREB to the F-SMS-CRE indicates that CREB binds cooperatively to the F-SMS-CRE. This sigmoidal curve, which is observed at low affinities, has been seen by others (Anderson & Dynan, 1994; Yin & Gaynor, 1996). The Hill plot analysis shows that CREB binds with both positive and negative cooperativity to the SMS-CRE. These binding characteristics are similar to these shown for the binding of nicotinamide adenine dinucleotide (NAD) to yeast glyceraldehyde 3-phosphate dehydrogenase (GAPDH) (Cook & Koshland, 1970; Bell & Dalziel, 1975; Cornish-Bowden and Koshland, 1975). In this situation, 2 mol of NAD bind to a tetramer of GAPDH with positive cooperativity. When the first two binding sites are occupied, there occurs a conformational change in which the affinity for NAD^+ for sites three and four are greatly reduced resulting in the negative cooperative phase of binding (Bell & Dalziel, 1975). It was somewhat surprising to find that CREB appears to associate as a tetramer both in the presence and absence of a DNA template containing a CRE. Calculations of the major CREB F-SMS-CRE complex by Ferguson plot analysis, either in the absence or presence of a DNA template, indicate a molecular size of 172 kDa (Figure 5F), consistent with CREB existing as a tetramer that binds to two oligonucleotide duplexes (Figure 6 A). However, it is possible that CREB tetramer may bind to a single oligonucleotide complex (see Figure 6A). Kinetic off-rate analyses of CREB showed two major binding affinities, a rapid low-affinity interaction and a slow high-affinity interaction consistent with a situation in which the binding interactions are complex. These DNA binding characteristics of CREB were also found using the asymmetric upstream DNA element in the SMS promoter (SMS-UE), indicating that the complex binding interaction and tetramer formation are not unique to just the high affinity SMS-CRE but may be more universal to all CREs. Therefore, our results from both kinetic and Ferguson plot analysis indicate that CREB forms a tetramer that interacts with the CREs resulting in complex binding interactions and dual cooperativity.

Due to the complex nature of the binding interaction between CREB and the F-SMS-CRE, it is difficult to precisely determine the dissociation constants utilizing bimolecular kinetic analysis. Therefore, we chose to only analyze the high-affinity binding interaction as defined by the linear portion of the Scatchard plot (Figure 1D) or the slow off-rate (Figure 4B) for which we can apply bimolecular kinetic analysis. Even though the values for binding affinities

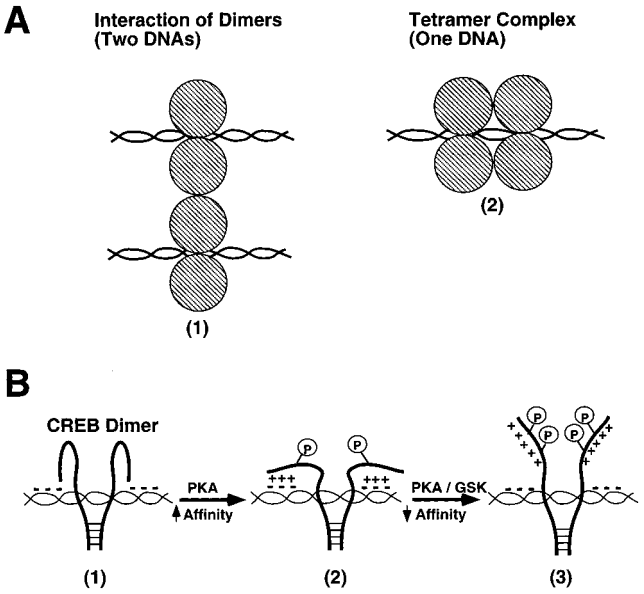

FIGURE 6: Models of CREB tetramers and the effect of phosphorylation of CREB on structure, net surface charge and DNA binding affinity. (A) Two possible models of the tetramerization of CREB. 1, Two CREB dimers, each binding independently to a DNA template, dimerize to form a tetrameric complex containing two DNA elements. 2, A tetrameric CREB complex binds to a single DNA template. (B) 1, CREB (depicted as a dimer) binds to the CRE with N-terminal sequences acting to destabilize binding. 2, Phosphorylation by PKA (P) alters conformation and increases the positive net surface charge (+) of CREB resulting in an increase in binding affinity by removing the destabilizing effect of the N-terminal amino acids. 3, Processive phosphorylation by GSK-3 results in a further alteration in conformation and an increase in positive net surface charge resulting in a destabilization of binding.

derived by this method may not reflect the true binding affinities due to the complex nature of the binding interactions, it seems reasonable to assume that the relative changes due to the mutations or phosphorylations determined by this method reflects important biological consequences. Even so, the dissociation constant of 11.1 nM derived from the least squares linear regression analysis of this line is consistent with other values reported for the binding of CREB to the SMS-CRE utilizing other methods of analyses (Hagiwara et al., 1993; Williams et al., 1993; Anderson & Dynan, 1994; Richards et al., 1996; Yin & Gaynor, 1996). However, the effects on other parameters, which we did not analyze, such as the effects on the fast dissociation rate and cooperativity may also reflect important effects of the binding of CREB to CREs.

Amino acids located at a distance from the DNA binding domain can influence the binding affinity for cognate DNA elements (Dombroski et al., 1993; Hunger et al., 1994; Roberts & Green, 1994). Previous experiments have suggested that sequences within the amino-terminal transactivation domain of CREB may be required for high affinity DNA binding (Vallejo et al., 1992). Deletion mutations that were tested in the fluorescent gel shift assay revealed that regions within the transactivation domain are responsible for high affinity DNA binding. Removal of the Q1 region of CREB (amino acids 1−91) resulted in a slight but significant increase in DNA binding affinity, suggesting that this region contains a binding destabilization region. Similar to CREB, N-terminal amino acids within the σ-factor and hepatic leukemia factor inhibit DNA binding, suggesting that a intermolecular interaction between amino acids within the N-terminal and DNA binding domains destabilize DNA binding (Dombroski et al., 1993; Hunger et al., 1994). Removal of an additional 25 amino acids into the P-box, deleting the PDE-1 domain and both GSK-3 and PKA sites, resulted in a dramatic reduction of greater than 20-fold in binding affinity indicating that the P-box is an important site for the regulation of DNA binding. More precise deletions of the P-box showed that the PDE-1 (amino acids 92−108) and PDE-3 (amino acids 131−148) domains but not the PDE-2 (amino acids 121−131) are critical regions for high-affinity binding. Deletions within the Q2 region resulted in a significant reduction in binding affinity probably reflecting the importance of the spacing between the P-box and bZIP region. Interestingly, removal of the entire transactivation domain resulted in a 2-fold increase in binding affinity, further supporting the notion that the N-terminal transactivation region of CREB contains a binding destabilization region. This last observation helps explain why the dominant negative inhibitors, ICER (inducible cAMP early repressor) and I-CREB (inhibitor of CREB), which are expressed at lower molar amounts can have significant effects on transcription due to their higher affinity of binding then the full length factors (Molina et al., 1993; Walker et al., 1996). Recent experiments have shown that I-CREB binds better to the CREs within the CREB promoter than full length CREB suggesting that DNA sequence specificity plays an important role in selecting various forms of CREB (Walker et al., 1996). Most importantly, these experiments demonstrate that CREB is not strictly a bipartite molecule and that amino acids within the P-box are not only necessary for regulating transactivation but also are required to stabilize DNA binding.

The importance of the PDE-1 domain in providing for high-affinity binding was intriguing since it contains many potential phosphorylation sites. The PDE-1 domain juxtaposes the GSK-3 site at serine 115 and PKA site at serine 119 on the amino-terminal side and contains five serines lying in consensus CKII phosphorylation sites. This arrangement is reminiscent of hierarchical phosphorylation sites in which multiple phosphorylations are interdependent on each individual phosphorylation (Kuenzel & Krebs, 1985; Roach, 1991; Henry & Killilea, 1993). We proposed that an initial phosphorylation of serine 119 by PKA would lead to the processive phosphorylation of serine 115 by GSK-3 and then subsequent phosphorylations within the PDE-1 domain by CKII. Fiol et al. had previously shown that processive phosphorylation between PKA and GSK-3 occurs in CREB and is important for transcriptional activation (Fiol et al., 1994). Our in vitro phosphorylation experiments of CREB confirmed these findings; however, we did not detect any further processive phosphorylation within the PDE-1 domain by CKII. CKII phosphorylated CREB within the PDE-1 domain in the absence of PKA and GSK-3 and is not involved in this processive kinase cascade. These results do not rule out the involvement of the serines within the PDE-1 domain as potential processive phosphorylation sites. de Groot et al. has shown that in the related transcription factor CREM, which contains a P-box with nearly identical amino acid sequences to CREB, the processive phosphory-

lation between PKA and GSK-3 occurs in vitro (de Groot et al., 1993). They also showed that CKII independently was a processive kinase with casein kinase I (CKI) within the a region similar to the PDE-1 domain. Interestingly, phosphorylation of CREM by both CK I and CK II resulted in an increase in binding affinity for the SMS-CRE (de Groot et al., 1993). Therefore, CKI or other kinases may play important roles in initiating a processive phosphorylation cascade within the P-box of CREB. Interestingly, we also showed that GSK-3 phosphorylates a site within the PDE-1 domain and, therefore, may be important for regulating binding and structure. These results indicate that, dependent on the state of a cell and the signals in receives from the environment, CREB can be multiply phosphorylated within the P-box, which would not only result in altered transcriptional activation but may influence DNA binding.

Whether phosphorylation of CREB can alter the ability to bind its cognate DNA elements has been controversial. Some groups have reported that PKA phosphorylation will enhance the binding especially to asymmetric low-affinity elements (Weih et al., 1990; Meinkoth et al., 1991; Nichols et al., 1992; de Groot et al., 1993) while others found that there was no effect of phosphorylation on DNA binding (Hagiwara et al., 1993; Richards et al., 1996). Our detailed analysis using both equilibrium and kinetic binding assays show that PKA enhances DNA binding by approximately 3−5-fold to both the high-affinity SMS-CRE and the lower affinity asymmetric CRE located within SMS-UE. Even though these changes are small, we feel that they will have important biological significance especially with binding to low-affinity sites. It was previously reported that the theoretical concentration of CREB within PC12 cell nuclei was 400 nM (Hagiwara et al., 1993), thus small changes in binding affinity of a high-affinity site (K_d = 1 to 10 nM) will probably have little consequence; however, with the low-affinity sites (> 100 nM), the effect of phosphorylation could be significant. We were curious to see that the elegant approach of detecting CREB−CRE binding interactions by use of fluorescent polarization provided no evidence for PKA induced DNA binding (Richards et al., 1996). Our only explanation to the discrepancy between these studies and ours is that the fluorescent polarization measurements were calculated assuming that there are no changes in protein conformation (Lundblad et al., 1996). The 3% increase in spherical size due to PKA phosphorylation, which we determined by Ferguson plot analysis, may have skewed the polarization data. The observation that processive kinase GSK-3 attenuated the PKA-enhanced binding was surprising to us, considering that GSK-3 synergistically enhances PKA mediated gene transcription from the somatostatin promoter (Fiol et al., 1994). However, as stated above, the effects of phosphorylation on the high affinity binding sites would not likely be detected and probably not play a major role in the regulation of CREB by GSK-3 on the somatostatin promoter in UF9 cells. We believe that GSK-3 phosphorylation of CREB can play an important role in regulating gene expression, especially on low-affinity sites, by attenuating the effect of PKA on DNA binding. Therefore, we conclude that phosphorylation of CREB by the processive kinases PKA and GSK-3 can alter the binding affinity for CREB to its CREs, and its biological significance will depend on the DNA element. The ability for CREB to initiate efficient transcription will therefore be dependent on the state of the signaling within the cell. Phosphorylation at serine 119 by the various signaling pathways, including the cAMP cascade, will favor high-affinity binding while signaling pathways that phosphorylation serine 115 will act to downregulate DNA binding and thus transcription.

Allosteric changes in conformation of CREB by phosphorylation has been proposed as a mechanism for regulating gene expression (Yamamoto et al., 1990; Gonzalez et al., 1991; Brindle et al., 1993; Lee & Masson, 1993). Protease digestion studies have suggested that PKA-induced alteration in conformation of both CREB and CREM plays a role in the induction of transcriptional activation (Gonzalez et al., 1991; Brindle et al., 1993). However, another study using protease digestion mapping and circular dichromism analysis has shown that phosphorylation at serine 133 does not effect the conformation of CREB (Richards et al., 1996). Interestingly, protease digestions studies on a related protein ATF1 demonstrated that phosphorylation alters its secondary structure (Masson et al., 1993). These experiments are limited, however, in that they only examine defined regions of the molecule, protease-sensitive regions and α-helical regions (circular dichromism), and do not look at the CREB/DNA complex as a whole in solution. Other techniques, such as NMR and X-ray crystallography, are also limited in the analysis of large protein/DNA complexes in solution. Therefore, we feel that Ferguson plot analysis when applied to DNA binding proteins can offer an opportunity to examine conformational changes associated with phosphorylation or other posttranslational modifications. The determination of the actual spherical sizes by Ferguson plot analysis are dependent on many assumptions, such as the degree of spherical nature of the CREB/DNA complex, the actual spherical sizes of the standards and the degree of hydration (Rodbard & Chrambach, 1971; Chrambach, 1985). This analysis has been shown to be accurate in determining molecular weights to within 5.6%, the error most likely due to the variability in the standards used to calculate the spherical size (Bryan, 1976). Since our experiments assess the relative changes in the spherical size of the same protein/DNA complex, we feel that the modest increase of 3.1 and 4.2% due to PKA and PKA/GSK-3 phosphorylation, respectively, reflects conformational changes in the CREB/DNA complex due to phosphorylation. Interestingly, our results also show that the amino acids within the P-box are important for maintaining the native conformation of CREB. Therefore, the Ferguson plot analysis gives us a unique way of detecting phosphorylation-induced changes in the conformation of the CREB/DNA complex in solution. These changes would thereby result in the alteration of the structural characteristics of CREB responsible for regulating DNA binding and transcriptional efficiency.

An important consequence of induced conformational changes would be an alteration of the charged amino acids that are involved in molecular interactions. A favored model of how phosphorylation of CREB induces the interaction with the CBP transcriptional co-activator is by providing a proper electrostatic environment (Parker et al., 1996; Richards et al., 1996). Results of the Ferguson plot analysis shows that PKA and PKA/GSK-3 phosphorylation dramatically effects the net surface charge of the CREB/DNA complex. Even though the actual charged values, protons per molecule, are

difficult to determine by this method (Rodbard & Chrambach, 1971; Chrambach, 1985), the relative changes due to phosphorylation are quite revealing. The major conclusion from these experiments is that phosphorylation at serine 119 and subsequently serine 115 results in an increase in positive net surface charge. This is significant since the inclusion of phosphate groups would be predicted to result in an addition of two negative charges at the pH used to run these gels. Phosphorylation-induced conformational changes could cause an increase in net surface charge by either exposing basic amino acids or masking negative acidic amino acids. The only charged regions within CREB lie within the P-box, a string of basic amino acids (PDE-2) flanked by a grouping of acidic amino acids (PDE-1 and 3) and the basic amino acids within the DNA binding domain. The mutational analysis of the PDE-1 domain indicated that these acidic domains are probably not the major contributors to the net surface charge. Whether the PDE-2, PDE-3, the DNA binding domains, or combinations of these domains are contributing to the net surface charge has not been determined. However, it is interesting to speculate that phosphorylation within the P-box would alter the conformation of CREB, thus, exposing the basic amino acids within the DNA binding domain and altering binding to the CREs. In fact, the changes in calculated net surface charge, due to the mutations in the PDE-1 domain, correlate with the binding affinities, an increase in positive net charge resulting in a decrease in binding affinity. Why the increase in positive net surface charge induced by PKA correlates with an increase in binding affinity is unclear; however, the further increase by GSK-3 does correlate with a decrease in binding affinity. Since we showed that GSK-3 can phosphorylate a site within the PDE-1 domain, the effect on binding affinity may be restricted to this region. Therefore, the changes in net surface charge may not strictly alter the binding affinities but have other yet undefined roles in regulating transcription. In conclusion, we present a model of how phosphorylation within the P-box of CREB can alter the binding affinity for cognate DNA elements by inducing an allosteric conformational change resulting in an alteration in the net surface charge (Figure 6B). Phosphorylation-induced structural changes would alter the intramolecular interaction of amino acids within the N-terminus and the sequences within the bZIP domain resulting in either stabilizing or destabilizing DNA binding directly or perhaps indirectly by altering dimerization. Our favored model would be that phosphorylation by PKA at serine 119 unmasks positive charges within the basic region of the DNA binding domain of CREB, thus, increasing its binding affinity to DNA. Subsequent phosphorylation by GSK-3 at serine 115 and within the PDE-1 domain would cause a further confirmational change resulting in interference in DNA binding or dimerization by the N-terminal region either by remasking the basic amino acids or by steric hinderance. Further support of our findings that phosphorylation of CREB alters its structure is provided by the studies of Radhakrishnan et al., in which phosphorylation of series 133 (equivalent to phosphoserine 119 in our description of CREB, see footnote 1) and is critical for the interactions of the pKID/p-box domain with the transcriptional coactivator CREB-binding protein, as determined by NMR spectroscopy (Radhakrishnan, 1997).

ACKNOWLEDGMENT

We thank Dr. Andreas Chrambach for analyzing the Ferguson plots with the RT/f, GIANTRUN, and CHARGE analysis programs and Dr. Ashook Khatri for synthesis of the fluorescent oligonucleotides. We also thank Holly Dressler and Monica Holbrook for help in the construction of the CREB mutants. Special thanks goes to Townley Budde for manuscript preparation and Drs. Mario Vallejo and William Walker for their constant support and critical analysis of this project. We also thank M.A. Weiss for a critical reading of the manuscript and helpful suggestions. J.F.H. is an investigator with the Howard Hughes Medical Institute. Supported in part by USPHS Grants DK30457 and DK25532.

REFERENCES

1. Anderson, M. G., and Dynan, W. S. (1994) *Nucleic Acids Res. 22*, 3194−3201.
2. Baker, R. E., Gabrielsen, O., and Hall, B. D. (1986) *J. Biol. Chem. 261*, 5275−5282.
3. Bell, J. E., and Dalziel, K. (1975) *Biochim. Biophys. Acta 410*, 243−251.
4. Berberich, S. J., and Cole, M. D. (1992) *Genes Dev. 6*, 166−176.
5. Brindle, P., Linke, S., and Montminy, M. R. (1993) *Nature 364*, 821−824.
6. Bryan, J. (1976) *Anal. Biochem. 78*, 513−519.
7. Chrambach, A. (1985) *The practice of quantitative gel electrophoresis*, Deerfield Beach, FL.
8. Chrivia, J. C., Kwok, R. P. S., Lamb, N., Hagiwara, M., Montminy, M. R., and Goodman, R. H. (1993) *Nature 365*, 855−859.
9. Cook, R. A., and Koshland, D. E. (1970) *Biochemistry 9*, 3337−3342.
10. Cornish-Bowden, A., and Koshland, D. E. (1975) *J. Mol. Biol. 95*, 201−212.
11. de Groot, R., Hertog, J., Vandenheede, J., Goris, J., and Sassone-Corsi, P. (1993) *EMBO J. 12*, 3903−3911.
12. Dombroski, A. J., Walter, W. A., and Gross, C. A. (1993) *Genes Dev. 7*, 2446−2455.
13. Ferguson, K. A. (1964) *Metab., Clin. Exp. 13*, 985−991.
14. Fiol, C. J., Mahrenholz, A. M., Wang, Y., Roeske, R. W., and Roach, P. J. (1987) *J. Biol. Chem. 262*, 14042−14048.
15. Fiol, C. J., Wang, A., Roeske, R. W., and Roach, P. J. (1990) *J. Biol. Chem. 265*, 6061−6065.
16. Fiol, C. J., Williams, J. S., Chou, C.-H., Wang, Q. M., Roach, P. J., and Andrisani, O. M. (1994) *J. Biol. Chem. 269*, 32187−32193.
17. Foulkes, N. S., Borrelli, E., and Sassone-Corsi, P. (1991) *Cell 64*, 739−749.
18. Fried, M., and Crothers, M. (1981) *Nucleic Acids Res. 9*, 6505−6525.
19. Ginty, D., Bonni, A., and Greenberg, M. (1994) *Cell 77*, 713−725.
20. Gonzalez, G. A., and Montminy, M. R. (1989) *Cell 59*, 675−680.
21. Gonzalez, G. A., Yamamoto, K. K., Fischer, W. H., Karr, D., Menzel, P., Biggs, W., Vale, W. W., and Montiminy, M. R. (1989) *Nature 337*, 749−752.
22. Gonzalez, G. A., Menzel, P., Leonard, J., Fischer, W. H., and Montminy, M. R. (1991) *Mol. Cell. Biol. 11*, 1306−1312.
23. Habener, J. F. (1990) *Mol. Endocrinol. 4*, 1087−1094.
24. Habener, J., Miller, C., and Vallejo, M. (1995) in *Vitamins and Hormones* (Litwack, G., Ed.) pp 1−5, Acedemic Press, San Diego, CA.
25. Hagiwara, M., Brindle, P., Harootunian, A., Armstrong, R., Rivier, J., Vale, W., Tsien, R., and Montminy, M. (1993) *Mol. Cell. Biol. 13*, 4852−4859.
26. Hai, T., Liu, F., Coukos, W. J., and Green, M. R. (1989) *Genes Dev. 3*, 2083−2090.

27. Hemmings, B. A., Aitken, A., Cohen, P., Rymond, M., and Hofmann, F. (1982) *Eur. J. Biochem. 127*, 473−481.
28. Henry, S., and Killilea, S. (1993) *Arch. Biochem. Biophys. 301*, 53−57.
29. Hill, A. V. (1910) *J. Physiol. 40*, iv−vii.
30. Hill, C. S., and Treisman, R. (1995) *Cell 80*, 199−211.
31. Hinkle, D. C., and Chamberlin, M. J. (1972) *J. Mol. Biol. 70*, 187−195.
32. Hoeffler, J. P., Meyer, T. E., Yun, Y., Jameson, J. L., and Habener, J. F. (1988) *Science 242*, 1430−1433.
33. Hoeffler, J. P., Lustbader, J. W., and Chen, C.-Y. (1991) *Mol. Endocrinol. 5*, 256−266.
34. Hunger, S. P., Brown, R., and Cleary, M. L. (1994) *Mol. Cell. Biol. 14*, 5986−5996.
35. Hunter, T., and Karin, M. (1992) *Cell 70*, 375−387.
36. Jain, N., Mahendran, R., Philp, R., Guy, G. R., Tan, T. H., and Cao, X. (1996) *J. Biol. Chem. 271*, 13530−13536.
37. Kapiloff, M., Farkash, Y., Wegner, M., and Rosenfield, M. (1991) *Science 253*, 786−789.
38. Kuenzel, E. A., and Krebs, E. G. (1985) *Proc. Natl. Acad. Sci. U.S.A. 82*, 488−492.
39. Kwok, R. P. S., Lundblad, J. R., Chrivia, J. C., Richards, J. P., Bachinger, H. P., Brennan, R. G., Roberts, S. G. E., Green, M. R., and Goodman, R. H. (1994) *Nature 370*, 223−226.
40. Lee, K. A. W., and Masson, N. (1993) *Biochim. Biophys. Acta 1174*, 221−233.
41. Lin, A., Frost, J., Deng, T., Smeal, T., Al-Alawi, N., and Karin, M. (1992) *Cell 70*, 777−789.
42. Lundblad, J. R., Laurance, M., and Goodman, R. H. (1996) *Mol. Endocrinol. 10*, 607−612.
43. Luscher, B., Christenson, E., Litchfield, D. W., Krebs, E. G., and Eisenman, R. N. (1990) *Nature 344*, 517−521.
44. Manak, J. R., and Prywes, R. (1991) *Mol. Cell. Biol. 11*, 3652−3659.
45. Manak, J. R., deBisschop, N., Kris, R. M., and Prywes, R. (1990) *Genes Dev. 4*, 955−967.
46. Masson, N., John, J., and Lee, K. A. W. (1993) *Nucleic Acids Res. 21*, 4166−4173.
47. Meinkoth, J. L., Montminy, M. R., Fink, J. S., and Feramisco, J. R. (1991) *Mol. Cell. Biol. 11*, 1759−1764.
48. Merino, A., Buckbinder, L., Mermelstein, F. H., and Reinberg, D. (1989) *J. Biol. Chem. 264*, 21266−21276.
49. Molina, C., Foulkes, N., Lalli, E., and Sassone-Corsi, P. (1993) *Cell 75*, 875−886.
50. Nichols, M., Weih, F., Schmid, W., DeVack, C., Kowenz-Leutz, E., Luckow, B., Boshart, M., and Schutz, G. (1992) *EMBO J. 11*, 3337−3346.
51. Parker, D., Ferreri, K., Nakajima, T., LaMorte, V. J., Evans, R., Koerber, S. C., Hoeger, C., and Montminy, M. R. (1996) *Mol. Cell. Biol. 16*, 694−703.
52. Rabault, B., and Ghysdael, J. (1994) *J. Biol. Chem. 269*, 28143−28151.
53. Richards, J., Bächinger, H., Goodman, R., and Brennan, R. (1996) *J. Biol. Chem. 271*, 13716−13723.
54. Riggs, A. D., Bourgeois, S., and Cohn, M. (1970) *J. Mol. Biol. 53*, 401−417.
55. Roach, P. J. (1991) *J. Biol. Chem. 266*, 14139−14142.
56. Roberts, S. G. E., and Green, M. R. (1994) *Nature 371*, 717−720.
57. Rodbard, D., and Chrambach, A. (1971) *Anal. Biochem. 40*, 95−134.
58. Sambrook, J., Fritsch, E. F., and Maniatis, T., Ed. (1989) *Molecular cloning, a laboratory manual*, Cold Spring Harbor Laboratory Press, Plainview, NY.
59. Sanger, F., Niklen, S., and Coulson, A. R. (1977) *Proc. Natl. Acad. Sci. U.S.A. 74*, 5463−5467.
60. Santiago-Rivera, Z., Williams, J., Gorenstein, D., and Andrisani, O. (1993) *Protein Sci. 2*, 1461−1471.
61. Scatchard, G. (1949) *Ann. N. Y. Acad. Sci. 51*, 660−672.
62. Segil, N., Roberts, s., and Heintz, N. (1991) *Science 254*, 1814−1816.
63. Sheng, M., Thompson, M., and Greenberg, M. (1991) *Science 252*, 1427−1430.
64. Smolik, S. M., Rose, R. E., and Goodman, R. H. (1992) *Mol. Cell. Biol. 12*, 4123−4131.
65. Stone, S. R., Hughes, M. J., and Jost, J.-P. (1991) *BioMethods*, pp 163−185, Birkhauser Verlag, Basal.
66. Tan, Y., Rouse, J., Zhang, A., Cariati, S., Cohen, P., and Comb, M. (1996) *EMBO J. 15*, 4629−4642.
67. Vallejo, M., Miller, C., and Habener, J. (1992a) *J. Biol. Chem. 267*, 12868−12875.
68. Vallejo, M., Penchuk, L., and Habener, J. F. (1992b) *J. Biol. Chem. 267*, 12876−12884.
69. Walker, W., Girardet, C., and Habener, J. (1996) *J. Biol. Chem. 271*, 20145−21050.
70. Weih, F., Stewart, A. F., Boshart, M., Nitsch, D., and Schutz, G. (1990) *Genes Dev. 4*, 1437−1449.
71. Williams, J. S., Dixon, J. E., and Andrisani, O. M. (1993) *DNA and Cell Biology*, pp 183−190, Mary Ann Liebert, Inc.,
72. Wilson, B., Mochon, E., and Boxer, L. (1996) *Mol. Cell. Biol. 16*, 5546−5556.
73. Wong, I., and Lohman, T. M. (1993) *Proc. Natl. Acad. Sci. U.S.A. 90*, 5428−5432.
74. Yamamoto, K., Gonzalez, G., Biggs III, W., and Montminy, M. (1988) *Nature 334*, 494−498.
75. Yamamoto, K. K., Gonzalez, G. A., Menzel, P., Rivier, J., and Montminy, M. R. (1990) *Cell 60*, 611−617.
76. Yin, M. J., and Gaynor, R. B. (1996) *Mol. Cell. Biol. 16*, 3156−3168.
77. Radhakrishnan, I., Perez-Alvarado, G. C., Parker, D., Dyson, H. J., Montminy, M. R., and Wright, P. E. (1997) *Cell* 91, 741−752.

BI970982T